

Supporting Information for ”’Seeing’ beneath the clouds - machine-learning-based reconstruction of North African dust events”

Franz Kanngießer¹ * and Stephanie Fiedler¹ †

¹Institute of Geophysics and Meteorology, University of Cologne, DE-50923 Cologne, Germany

Contents of this file

1. Figures S1 to S5
2. Tables S1 to S2

References

Sun, W., Videen, G., Kato, S., Lin, B., Lukashin, C., & Hu, Y. (2011). A study of subvisual clouds and their radiation effect with a synergy of CERES, MODIS, CALIPSO, and AIRS data. *Journal of Geophysical Research: Atmospheres*, 116(D22). doi: [_____](#)

Corresponding author: F. Kanngießer fkanngiesser@geomar.de

* current address, GEOMAR Helmholtz

Center for Ocean Research Kiel, DE-24105

Kiel, Germany

† current address, GEOMAR Helmholtz

Center for Ocean Research Kiel, DE-24105

Kiel, Germany and Christian-Albrechts

University of Kiel, DE-24118 Kiel, Germany

X - 2

KANGIESSER AND FIEDLER: "SEEING" BENEATH THE CLOUDS

10.1029/2011JD016422

Dust occurrence frequency (%) at 12 UTC (2021)

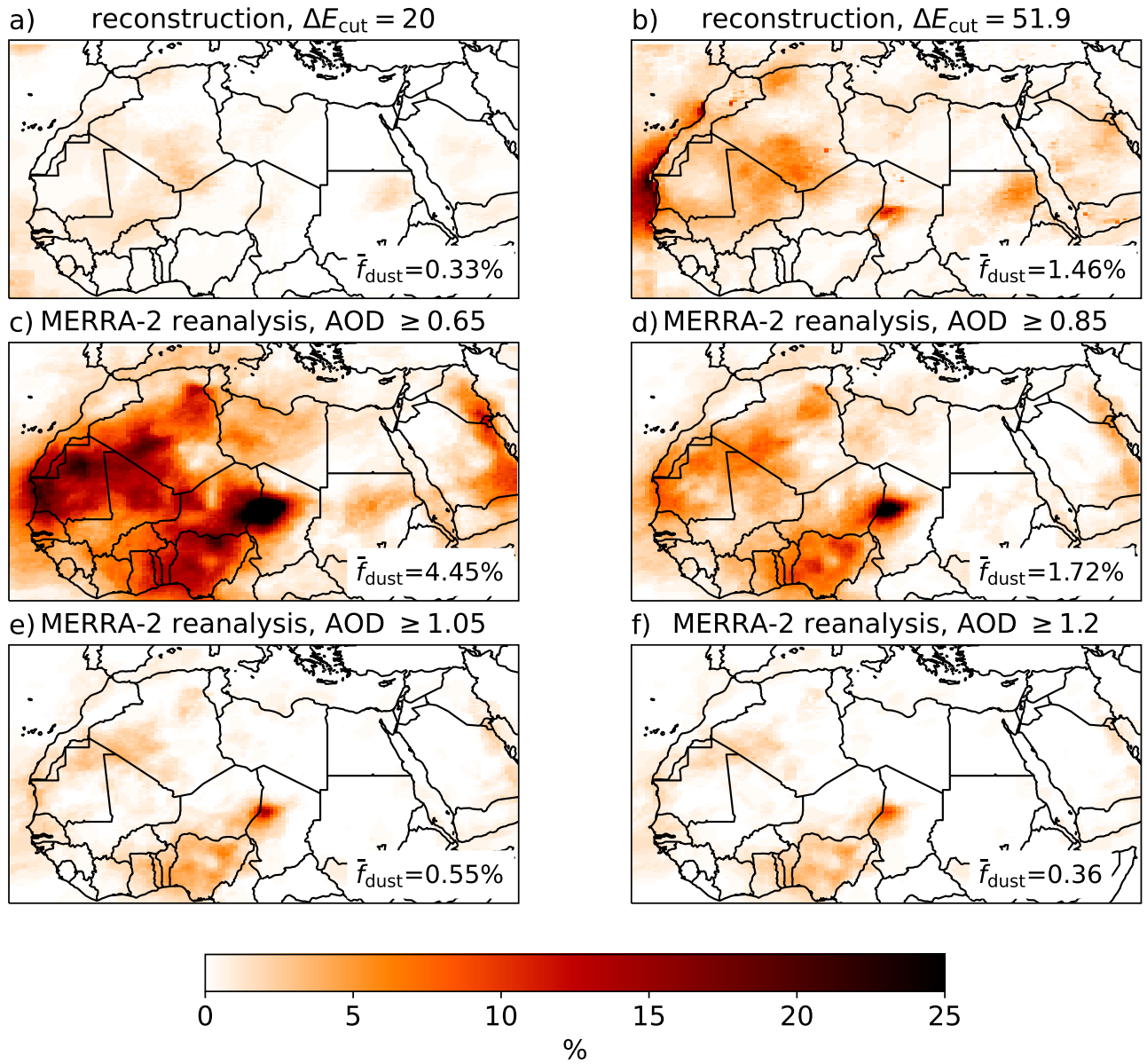


Figure S1. Comparison of dust occurrence frequency in 2021 from reconstruction with different values of ΔE_{cut} (top row) and from MERRA-2 reanalysis with different lower bounds of dust AOD (middle and bottom row).

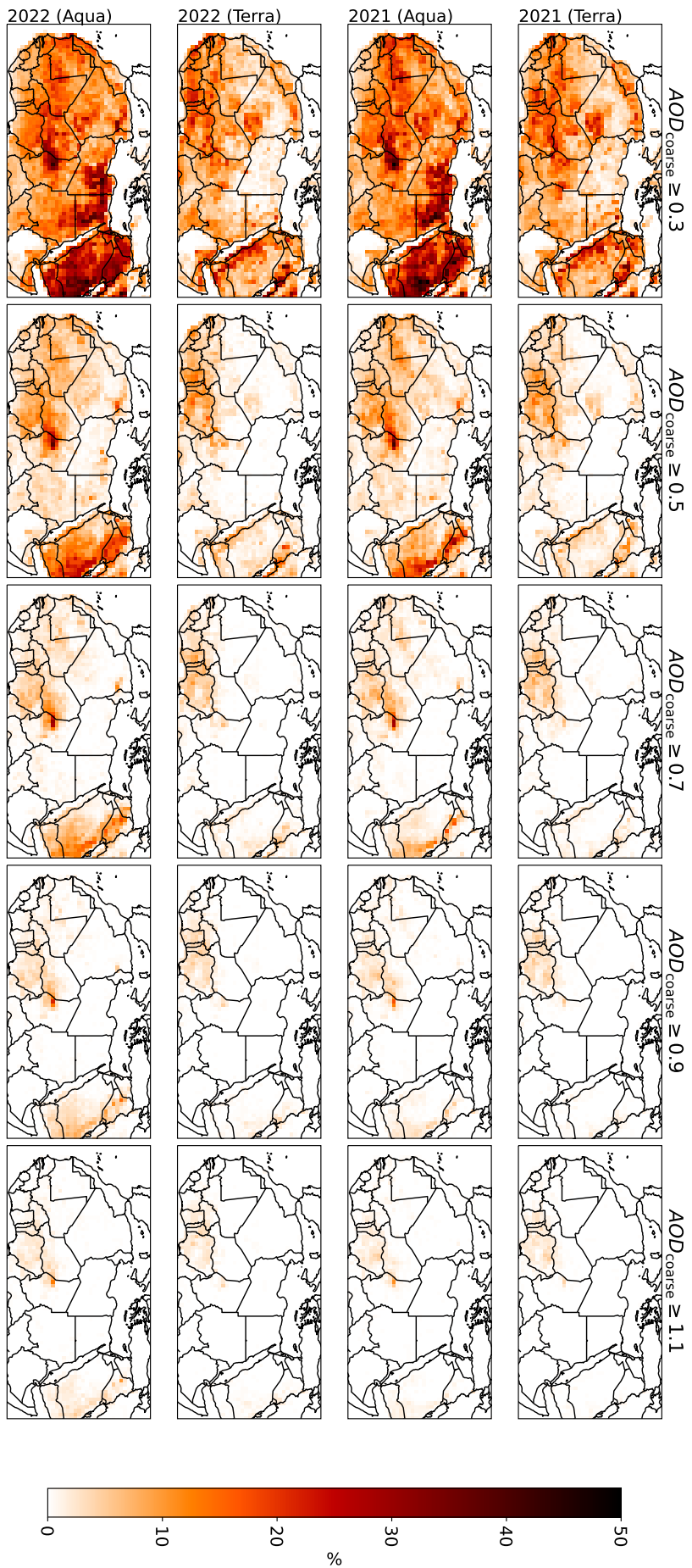


Figure S2. Coarse particle occurrence frequency derived from MODIS level 3 data for different thresholds of AOD (columns) in 2021 (top two rows) and 2022 (bottom two rows). The first and third row show data from MODIS/Terra, the second and fourth row from MODIS/Aqua.

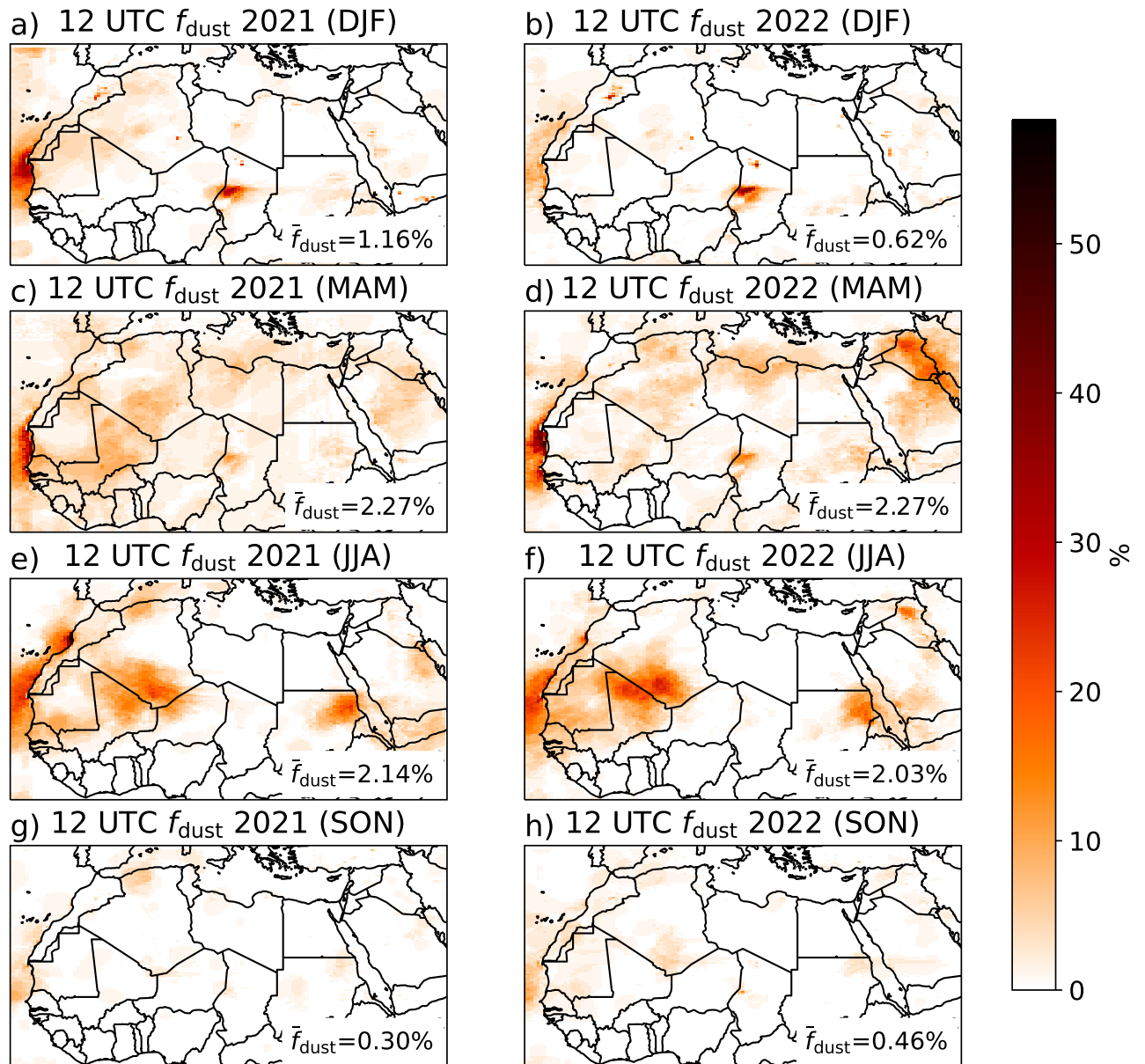


Figure S3. Reconstructed seasonal dust occurrence frequencies with $\Delta E_{\text{cut}} = 51.9$ in 2021 (left column) and 2022 (right column). Rows indicate the season.

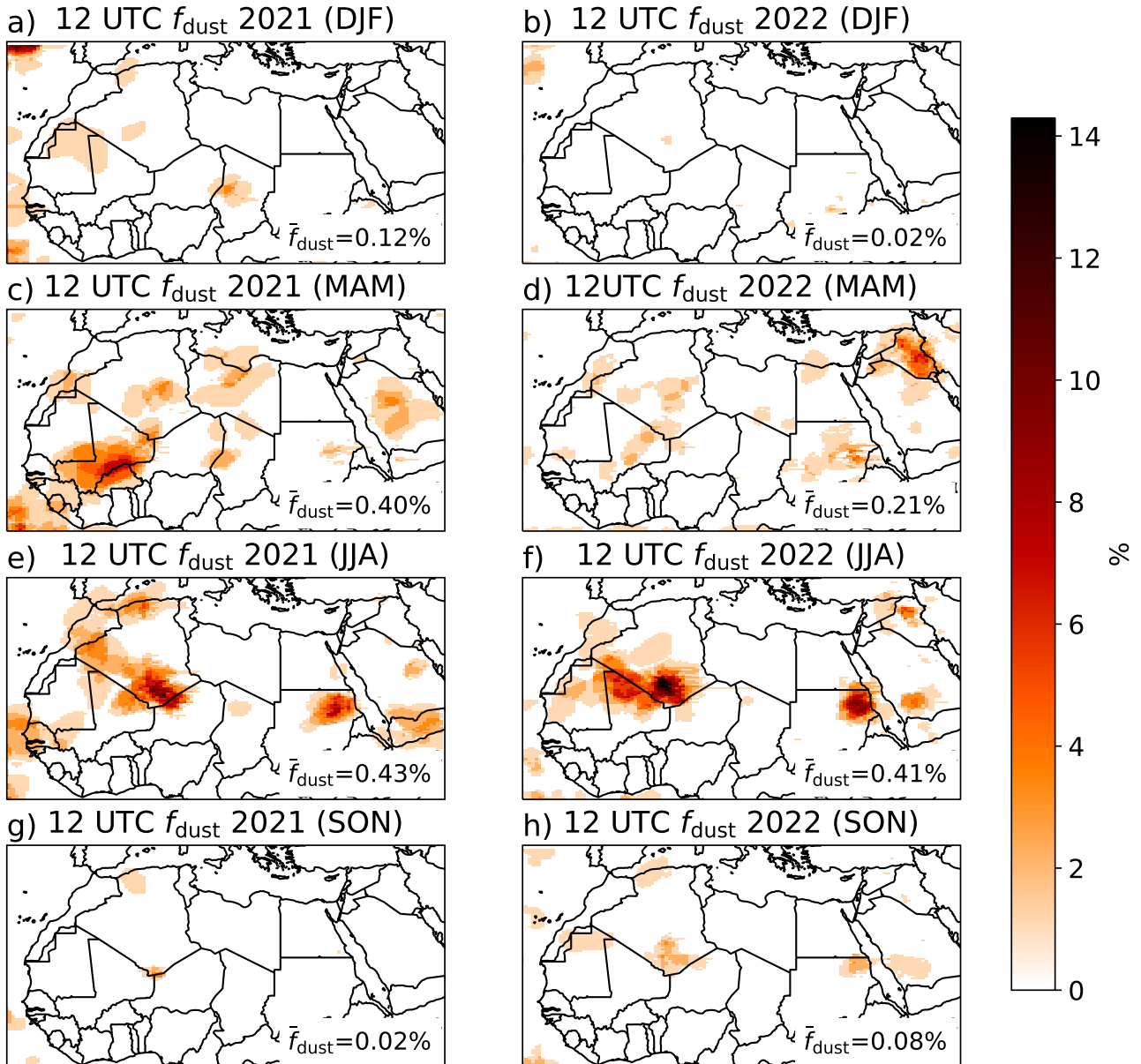


Figure S4. As Fig. S3, but with $\Delta E_{\text{cut}} = 20.0$.

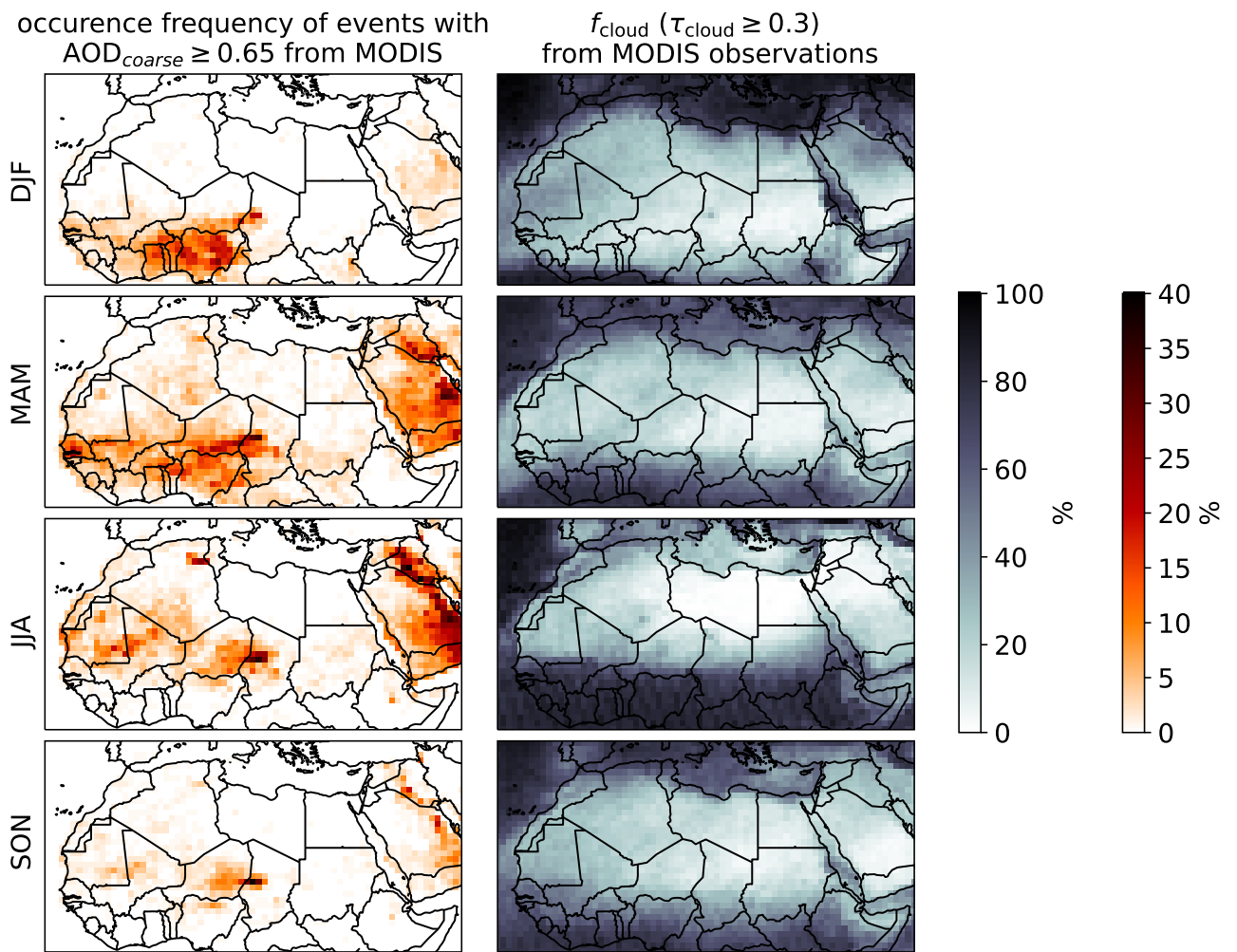


Figure S5. Seasonal occurrence frequency of events with $AOD_{coarse} \geq 0.65$ (left column) and cloud occurrence frequency f_{cloud} . Clouds are defined as pixels with values of cloud optical depth of $\tau_{cloud} \geq 0.3$ (cf. Sun et al., 2011).

Table S1. Overview over the first, second and third quartiles of the different similarity measures, SSIM, directed Hausdorff distance (HD), and PSNR between the dust event reconstruction and the individual numerical models in the ensemble provided by the WMO

Regional Center Barcelona for 2021. The quartiles are also indicated in Fig. 5.

model	Q_1 (SSIM)	Q_2 (SSIM)	Q_3 (SSIM)	Q_1 (HD)	Q_2 (HD)	Q_3 (HD)	Q_1 (PSNR)	Q_2 (PSNR)	Q_3 (PSNR)
ALADIN	0.7977	0.9291	0.9717	1.2071	2.8284	6.1235	10.3873	16.5752	23.2378
BSC-DREAM8b	0.9231	0.9584	0.9829	0.0000	1.7321	2.4495	16.1893	20.1203	25.4512
CAMS-IFS	0.8871	0.9286	0.9829	2.0000	2.8284	3.6056	15.3205	18.4613	22.8248
DREAM8-CAMS	0.9176	0.9561	0.9817	0.0000	1.8660	2.4495	16.4534	20.1166	25.1764
EMA-RegCM4	0.9168	0.9538	0.9795	0.0000	2.0000	2.6458	16.0858	19.5080	24.8203
ICON-ART	0.8375	0.9063	0.9615	1.4142	3.6056	4.6904	13.2737	15.7097	21.1405
LOTOS-EUROS	0.5763	0.6981	0.8096	5.8310	7.1414	7.9373	6.6788	8.9512	11.4620
MONARCH	0.6241	0.7088	0.8244	5.6569	7.2801	8.3066	7.3456	8.7101	11.6249
NASA-GEOS	0.8964	0.9333	0.9736	1.0000	2.6458	3.8730	14.9364	17.6418	22.8890
NCEP-GEFS	0.7140	0.8450	0.9136	3.4994	5.0000	6.7823	9.6400	13.4402	17.6882
NOA	0.7118	0.8838	0.9439	3.0000	4.8990	6.9282	8.6930	14.3754	18.5512
SILAM	0.8642	0.9006	0.9432	2.8284	3.7416	4.6904	13.2550	15.6025	18.6762
WRF-NEMO	0.8754	0.9597	0.9883	0.0000	1.4142	2.4495	13.8600	19.8911	30.3248
MULTI-MODEL	0.8925	0.9407	0.9761	0.0000	2.4495	3.8730	14.3954	17.9117	23.2233

Table S2. As Tab. S1, but for 2022

model	Q_1 (SSIM)	Q_2 (SSIM)	Q_3 (SSIM)	Q_1 (HD)	Q_2 (HD)	Q_3 (HD)	Q_1 (PSNR)	Q_2 (PSNR)	Q_3 (PSNR)
ALADIN	0.7815	0.8708	0.9341	2.4495	3.8730	5.8310	10.7707	14.2239	17.9710
BSC-DREAM8b	0.8816	0.9167	0.9473	0.0000	2.2361	2.8713	14.2320	16.3534	19.8397
CAMS-IFS	0.8608	0.9115	0.9525	2.4495	3.4641	4.4721	14.0251	16.6665	20.6829
DREAM8-CAMS	0.9005	0.9486	0.9735	1.4142	2.0000	2.6914	15.6048	19.4258	24.7018
EMA-RegCM4	0.8859	0.9159	0.9456	1.0000	2.2361	3.1623	14.4719	16.9855	19.7826
ICON-ART	0.8481	0.9250	0.9697	1.0000	3.0000	4.7958	13.4285	17.0254	23.4519
LOTOS-EUROS	0.6153	0.6978	0.8043	5.7446	7.0000	7.8103	7.0981	8.6572	11.4884
MOCAGE	0.9084	0.9633	0.9838	0.0000	2.0000	2.8285	15.6998	20.8732	26.1290
MONARCH	0.6657	0.7601	0.8517	4.4721	6.5574	7.8103	8.0428	9.9274	13.7622
NASA-GEOS	0.8232	0.9067	0.9629	2.0000	3.6056	4.8990	12.0582	15.6509	21.4623
NCEP-GEFS	0.8762	0.9272	0.9676	1.7321	2.8284	4.0000	14.3555	17.4460	22.1660
NOA	0.7370	0.8129	0.8941	4.0616	5.1961	6.0828	9.3595	11.8748	15.4327
SILAM	0.8667	0.9220	0.9703	1.4142	2.8284	4.1829	13.9209	17.1405	22.8890
WRF-NEMO	0.8559	0.9011	0.9313	0.0000	1.7321	3.1623	13.5709	15.8400	18.0831
ZAMG-WRF-CHEM	0.7304	0.8167	0.9097	3.8730	5.4312	6.4807	9.7896	12.3261	17.3824
MULTI-MODEL	0.8841	0.9431	0.9750	0.0000	2.2361	3.6056	14.3845	18.3602	23.8191